Development of a 60 GHz Millimeter-Wave Wireless Transmission System for the CEPC Inner Tracker Detector

Jun Hu and Chongyao Song

***Abstract*—The high-speed data readout in the Inner Tracker (ITK) of the Circular Electron-Positron Collider (CEPC) faces severe signal density and space constraints, driving the need for wireless readout solutions that combine low material budget, high data rate, and radiation tolerance. This paper presents the development and experimental validation of a 60 GHz millimeter-wave (mm-Wave) wireless transmission system based on the commercial off-the-shelf (COTS) ST60A2 chip. Radiation tolerance tests were conducted under both X-ray Total Ionizing Dose (TID) and neutron Non-Ionizing Energy Loss (NIEL) conditions, confirming that the core chip can withstand a TID exceeding 5 Mrad and a 1 MeV equivalent neutron fluence of 1.2×10^{12} n_{eq}/cm^2 without performance degradation. Through link budget analysis, a power amplifier (PA) with 19 dB gain was introduced, extending the effective transmission distance to 45 cm at a data rate of 5 Gbps. The enhanced mm-Wave transceiver module measures only 14 mm $\times$ 9 mm, integrating the ST60A2, the PA, and a PCB patch antenna. No electromagnetic interference was observed between the mm-Wave link and the CEPC pixel prototype chip TAICHU3. A six-channel wireless transmission system was further constructed using flexible printed circuit (FPC) technology. experimental results demonstrate an aggregated data rate of 18.75 Gbps (6 channels $\times$ 3.125 Gbps) over a transmission distance of 10–30 cm with a bit error rate (BER) below 10^{-13}. The results confirm the engineering viability of 60 GHz mm-Wave technology for ITK readout and provide a practical reference for wireless data transmission in next-generation high-energy physics experiments.**

***Index Terms*—CEPC, millimeter-wave transmission, 60 GHz, radiation tolerance, wireless readout, high-energy physics experiment**

I. Introduction

THE Circular Electron-Positron Collider (CEPC) is a next-generation high-energy physics facility planed to operate at a center-of-mass energy of 240 GeV, producing millions of Higgs bosons and enabling precision studies of the Standard Model and electroweak interactions [1]. The CEPC reference detector includes a silicon-based Inner Tracker (ITK) located between the vertex detector and the Time Projection Chamber (TPC), which provides precise charged-particle trajectory measurements [1].

In the high-luminosity Higgs operation mode, the ITK produces a large data volume. Each stave of the ITK barrel structure carries 14 sensor modules with an raw data rate of approximately 1.2 Gbps [1], With 210 staves in total across three barrel layers, the overall data volume presents a significant readout challenge. Traditional wired or optical-fiber readout schemes introduce substantial material budget, which degrades tracking resolution through multiple scattering and energy loss of traversing particles. Furthermore, dense cable routing also complicates detector assembly and maintenance, and radiation-induced degradation limits long-term reliability.

To address these challenges, wireless data transmission has been proposed as an alternative readout paradigm for particle physics detectors [2]–[7]. Concurrent studies have also explored the mechanical constraints associated with ultra-light detector support structures [8]. Among the candidate technologies, the 60 GHz millimeter-wave band (57–66 GHz) offers several compelling advantages: (1) a wide available bandwidth of up to 9 GHz supporting multi-Gbps data rates; (2) a short wavelength of approximately 5 mm, enabling antenna miniaturization and on-chip integration; (3) strong directionality that naturally suppresses inter-channel interference; and (4) high atmospheric attenuation that further reduces crosstalk between adjacent detector subsystems [9].

Despite these advantages, several critical engineering bottlenecks remain unresolved for the application of 60 GHz technology in high-energy physics detectors. First, the radiation tolerance of commercial mm-Wave chips in the harsh CEPC environment has not been systematically validated. The annual TID reaches 5 Mrad and the 1 MeV equivalent neutron fluence approaches 0.97×10^{12} n_{eq}/cm^2 [12]. Second, the limited output power of a single COTS mm-Wave chip limits the transmission distance, which must satisfy the inter-layer spacing of 11–21 cm in the CEPC ITK. Third, the integration of multiple mm-Wave channels within the compact detector volume while maintaining signal integrity, has not been demonstrated.

This paper addresses these gaps through a systematic development and verification program. The main contributions are: (1) combined TID and NIEL radiation tolerance verification of the ST60A2 60 GHz chip under conditions representative of the CEPC environment; (2) link budget analysis and the design of an enhanced mm-Wave transceiver module that achieves 45 cm transmission distance at 5 Gbps; (3) single-channel performance characterization across multiple data rates with BER and eye-diagram analysis; and (4) a six-channel FPC-based wireless transmission system demonstrating 18.75 Gbps aggregated throughput with BER below 10^{-13}.

Corresponding author: Jun Hu.

Jun Hu and Chongyao Song are with the Institute of High Energy Physics, Chinese Academy of Sciences, Beijing,100049, China and University of Chinese Academy of Sciences, Beijing, 100049, China (e-mail: hujun@ihep.ac.cn)

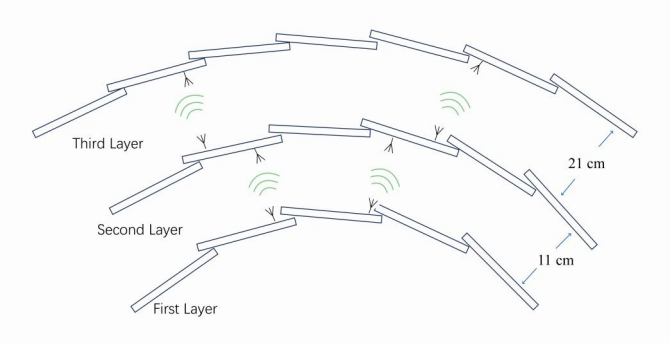

Fig. 1. Schematic of the CEPC radial wireless data transmission architecture. Data flows radially outward from the inner tracker layers through mm-Wave links, with optional relay stages.

This paper is organized as follows. Section II describes the system architecture and link budget analysis. Section III presents the radiation tolerance tests. Section IV details the single-channel performance characterization. Section V describes the multi-channel system integration and test results. Section VI concludes the paper.

II. System Architecture and Link Budget

A. Wireless Readout Architecture

The CEPC detector features a cylindrical barrel structure with an inter-layer radial spacing of 11–21 cm. Fig. 1 shows the proposed wireless data transmission scheme. Data generated by the front-end electronics of the ITK is transmitted radially outward through a series of mm-Wave links. The architecture comprises three functional layers: the Transmission Layer mounted on the inner detector (e.g., ITK barrel staves), the Reception Layer installed on the outer detector structures (e.g., outermost staves, TPC or OTK support frames), and an optional Relay Layer that extends the transmission reach when inter-layer distances exceed single-hop capability.

This radial readout topology avoids the cable congestion that occurs when all connections converge at the detector endcaps, and significantly reduces the cumulative material budget by replacing copper conductors and optical fibers with contactless mm-Wave links.

B. Link Budget Analysis

The STMicroelectronics ST60A2 chip was selected as the core transceiver [10]. It operates in the 60 GHz band with Amplitude Shift Keying (ASK) non-coherent modulation, supporting data rates from 1 Mbps to 6.6 Gbps. The transmitter consumes 44 mW and the receiver 27 mW in active mode. The chip is housed in a VFBGA package measuring 2.2 mm $\times$ 2.2 mm $\times$ 0.8 mm, with SLVS and CMOS I/O interfaces.

A PCB patch antenna was designed and simulated for the 60 GHz band. It provides a gain of approximately 9 dBi with left-handed circular polarization (LHCP). The antenna radiation pattern exhibits a half-power beamwidth of roughly 70° in both the Phi = 0° and Phi = 90° planes, and cross-polarization discrimination better than 10 dB.

At 5 Gbps, the ST60A2 offers an intrinsic link budget of approximately 28 dB. Accounting for the 9 dBi antenna gain at both the transmitter and receiver, the total available link budget is:

$$\text{Link Budget}_{\text{total}} = 28 + 9 + 9 = 46 \text{ dB} \quad (1)$$

The free-space path loss (FSPL) at 60 GHz, including atmospheric oxygen absorption of approximately 15 dB/km [11], follows the Friis transmission equation:

$$\text{FSPL}(d) = 128.0 + 20\log_{10}\left(\frac{d}{1000}\right) + 0.015d \ \ [\text{dB}] \quad (2)$$

where d is the transmission distance in meters. Setting the total path loss to the available link budget:

$$128.0 + 20\log_{10}(d) - 20\log_{10}(1000) + 0.015d = 46 \quad (3)$$

Solving Eq. 3 gives a theoretical maximum transmission distance of approximately 8 cm. This falls short of the 11–21 cm inter-layer spacing required by the CEPC ITK, confirming the necessity of introducing a power amplifier (PA) to boost the transmitted signal.

For a 40 cm design target, the total path loss is calculated to be approximately 60.1 dB, exceeding the available 46 dB budget by 14.1 dB. Considering additional engineering margins including impedance mismatch loss, dielectric loss in PCB substrates, and installation de-tuning effects (cumulatively estimated at 5–10 dB), a PA providing approximately 19 dB of gain was selected.

C. Enhanced mm-Wave Transceiver Module

Fig. 2 shows the enhanced mm-Wave transceiver module. The module integrates the ST60A2 chip with a two-stage PA chain providing a gain of 19 dB at 60 GHz. A PCB patch antenna was adopted in place of a conventional horn antenna, enabling a compact form factor of 14 mm $\times$ 9 mm. The module features a stamp-hole edge connector interface for simplified integration with flexible printed circuits. Two module variants were fabricated: transmit module and receive module, sharing the similar PCB layout but differing in the signal flow direction and passive network configuration.

The module supports both Full Data Rate (FDR) differential mode (1 Mbps–5 Gbps) and High Data Rate (HDR) differential mode (200 Mbps–6.6 Gbps), configurable through hardware strap pins or an I^2C interface. The supply voltage is 1.8 V for the ST60A2 core and a separate supply rail for the PA stages.

III. Radiation Tolerance Tests

In the CEPC Higgs operation mode, the estimated radiation background includes a Total Ionizing Dose of approximately 5 Mrad per year and a 1 MeV equivalent neutron fluence of 0.97×10^{12} $n_{\text{eq}}/\text{cm}^2$ per year [12]. To assess the suitability of the ST60A2 chip for this environment, two radiation tests were performed: an X-ray TID test and a neutron NIEL test.

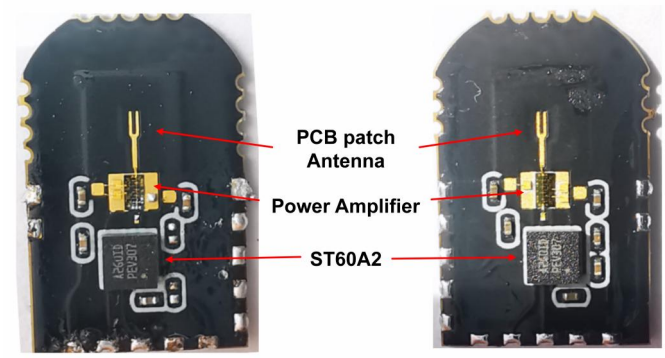

Fig. 2. Enhanced mm-Wave transceiver module integrating ST60A2, PA chain, and PCB patch antenna. (Left) Transmit module, (Right) Receive module. Dimensions: 14 mm × 9 mm.

Fig. 3. X-ray TID irradiation test setup at the MultiRad 160 facility.(Left) SK202 installed, (Right) enhanced modules installed

A. Total Ionizing Dose Test

The TID test was conducted at the Institute of High Energy Physics using a MultiRad 160 X-ray irradiation facility. The X-ray source was operated at a tube voltage of 40 kV and a tube current of 20 mA, with a 0.15 mm aluminum filter to attenuate low-energy spectral photons. The ST60A2 test board was positioned at a distance of 13 cm from the source, corresponding to a dose rate of 21,234 rad/min (Si equivalent), as calibrated using a reference diode. Under these conditions, the time required to accumulate a total dose of 5 Mrad was approximately 3.9 hours.

The ST60A2 test board (SK202 evaluation platform) was configured as a continuous 60 GHz communication link operating at 1 Gbps during the entire irradiation period. The link throughput was monitored in real time using the iperf3 network measurement tool over a TCP connection. The on-board power supply rails and the communication bandwidth were recorded throughout the test.

The chip sustained stable operation through the full 5 Mrad exposure. No link dropouts or significant throughput degradation were observed. The supply current consumption remained within the datasheet specifications, and the chip resumed normal operation immediately after irradiation without requiring power cycling. Additionally, the enhanced modules with external PA devices were co-tested and exhibited no gain degradation under the same TID exposure.

B. Non-Ionizing Energy Loss Test

The NIEL test was performed at the China Spallation Neutron Source (CSNS), which delivers an 80 MeV proton beam

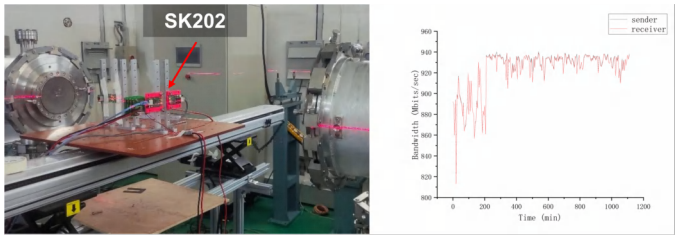

Fig. 4. Neutron NIEL irradiation test at CSNS. (Left) SK202 (ST60A2 test board) at the beamline; (Right) Communication bandwidth monitored during neutron irradiation.

TABLE I
RADIATION TOLERANCE SUMMARY OF THE 60 GHZ MM-WAVE COMPONENTS.

Device	TID (Mrad)	NIEL (10^{12} n_{eq}/cm^2)
ST60A2 (60 GHz chip)	>5	1.2
PA (power amplifier)	>5	not tested

onto a tungsten target to produce a white neutron spectrum. The neutron beam intensity at the irradiation position was 1.65×10^7 n_{eq}/cm^2/s, with a measured absorption coefficient of 0.95 for the ST60A2 package materials. The total irradiation duration was 21 hours, corresponding to an accumulated 1 MeV equivalent neutron fluence of approximately 1.2×10^{12} n_{eq}/cm^2, which exceeds the annual NIEL budget of the CEPC ITK region.

During the neutron irradiation, the ST60A2 communication link remained operational. Minor fluctuations in link bandwidth were observed, attributable to single-event transient effects in the chip's digital control logic, but no permanent link failures or latch-up events occurred. After completion of the full irradiation cycle, the chip was power-cycled and re-tested, confirming full functional recovery with communication performance identical to pre-irradiation levels.

Table I summarizes the radiation tolerance results for the ST60A2 chip and the associated PA devices.

These results provide the systematic radiation tolerance data for a COTS 60 GHz mm-Wave transceiver chip under combined TID and NIEL conditions representative of a next-generation particle physics detector environment.

IV. Single-Channel Performance Characterization

A. Test System Configuration

A dedicated single-channel test platform was developed to characterize the transmission performance of the enhanced mm-Wave module. Fig. 5 illustrates the test system architecture. The platform comprises a Xilinx Kintex-7 FPGA (xc7k325tffg676) evaluation board with an FMC High-Pin-Count (HPC) interface, a custom adapter board providing regulated 5 V power rails, and the mm-Wave transceiver test board equipped with an SFP connector interface for high-speed data injection and extraction.

For bit error rate (BER) characterization, the Xilinx iBert (Integrated Bit Error Ratio Tester) IP core was utilized. The iBert core instantiates a pseudo-random binary sequence

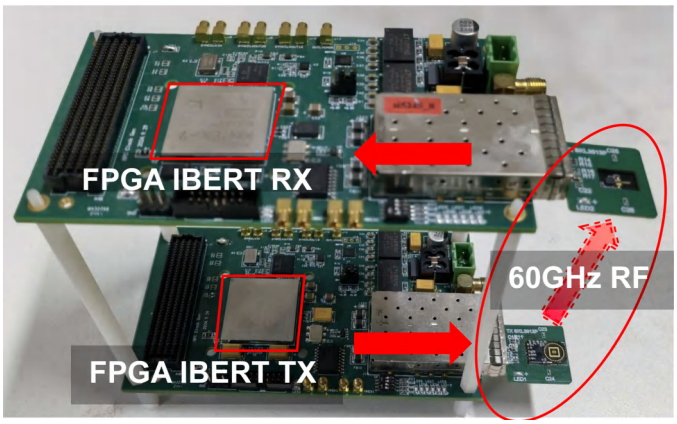

Fig. 5. Single-channel mm-Wave transmission test platform.

TABLE II
SINGLE-CHANNEL TRANSMISSION DISTANCE AND DATA RATE PERFORMANCE.

Data Rate (Gbps)	Stable Distance (cm)
1.25	67.5
4	50
5	45
6.6	22.5

(PRBS) pattern generator and checker within the FPGA fabric, driving the GTX multi-gigabit transceivers. The PRBS pattern is transmitted from the FPGA TX through the SFP interface to the transmit module, radiated across the free-space 60 GHz link, received by the receive module, and looped back to the FPGA RX for real-time error counting. The iBert configuration and BER readout are controlled through the Vivado Serial I/O Analyzer via the JTAG interface.

B. Transmission Distance and Data Rate

Table II presents the measured transmission performance of the enhanced mm-Wave module across four data rates. The "Stable Distance" is defined as the maximum distance at which BER remains below 10^{-13} over a measurement interval of at least 30 minutes.

The results demonstrate that the introduction of the 19 dB PA successfully extends the practical transmission range well beyond the CEPC inter-layer spacing requirement. At a data rate of 5 Gbps, a stable error-free distance of 45 cm is achieved, representing a greater than five-fold improvement over the 8 cm theoretical limit without amplification. At the nominal ITK requirement of 1.2 Gbps, the module readily supports transmission over distances exceeding 60 cm with ample margin.

C. Eye Diagram Analysis

Fig. 7 shows the eye diagram measured at the receiver output for a 5 Gbps PRBS-7 signal transmitted over 20 cm. The eye is wide and vertically clean, indicating sufficient timing margin and signal-to-noise ratio for robust clock-and-data recovery (CDR). The measured eye height is approximately

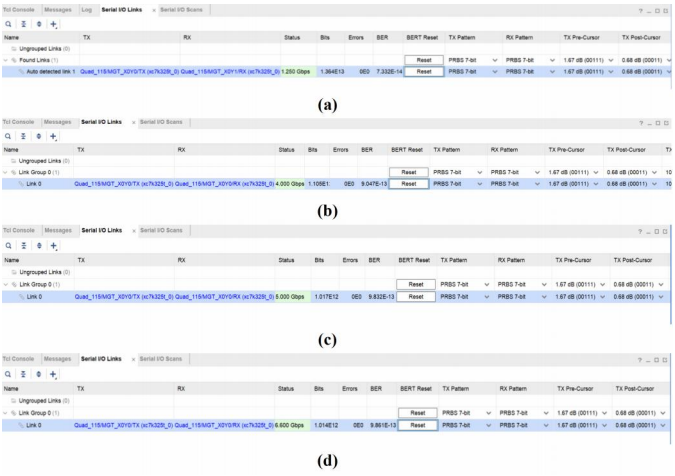

Fig. 6. BER vs. transmission distance at four data rates: (a) 1.25 Gbps, (b) 4 Gbps, (c) 5 Gbps, (d) 6.6 Gbps.

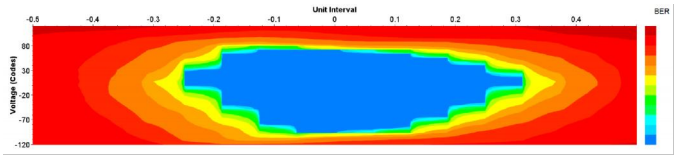

Fig. 7. Eye diagram measured at 5 Gbps, 20 cm transmission distance. Horizontal scale: 50 ps/div; vertical scale: 50 mV/div.

120 mV (differential) and the eye width exceeds 0.6 UI at a BER contour of 10^{-12}.

D. Alignment Tolerance and Penetration Capability

Misalignment tolerance tests were conducted to evaluate the sensitivity of the mm-Wave link to angular and lateral misalignment. The results indicate that the link remains stable with lateral offsets of up to ± 5 mm and angular misalignment of up to $\pm 10^{\circ}$ in both azimuth and elevation at a 3 cm separation distance. At larger distances (10–20 cm), the angular tolerance increases due to the diverging beam geometry.

Material penetration tests were carried out at a 10 cm separation distance with representative detector materials placed in the beam path. The results are summarized in Table III . Thin, low-permittivity materials such as paper, plastic sheet, and flex PCB substrate do not attenuate the 60 GHz link. Standard 1.6 mm FR4 PCB, however, completely blocks the signal, consistent with the high dielectric and conductor loss of FR4 at millimeter-wave frequencies.

E. Electromagnetic Compatibility with Detector Chip

To verify that the 60 GHz mm-Wave transmission does not interfere with the sensitive front-end detector electronics, an electromagnetic compatibility (EMC) test was performed with the TAICHU3 pixel sensor chip, which is a prototype CMOS pixel sensor designed for the CEPC vertex detector fabricated in a 180 nm process [13]. The TAICHU3 chip was operated in its nominal configuration, and its noise distribution and threshold distribution were measured both with and without

TABLE III
MATERIAL PENETRATION TEST AT 10 CM TRANSMISSION DISTANCE.

Material	Thickness (mm)	Link Status
Paper	2	Connected
Plastic	2	Connected
FR4 PCB	1.6	Blocked
Flex PCB	0.2	Blocked

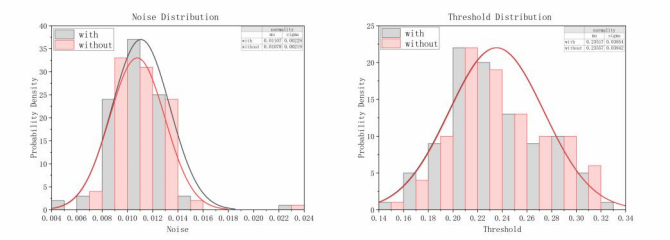

Fig. 8. The comparison between with and without mm-Wave. (Left) Noise distribution, (Right) threshold distribution

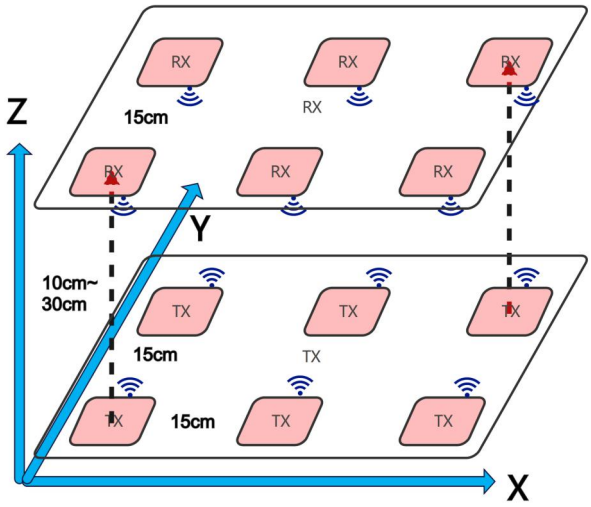

Fig. 9. Multi-channel mm-Wave transmission system architecture.

an active 60 GHz mm-Wave link positioned at a distance of 3 cm.

Fig. 8 shows the RMS noise was 0.0111V (mm-Wave on) versus 0.0108V (mm-Wave off), a difference within statistical uncertainty. The threshold spread after tuning was 0.2352V versus 0.2356V, showing no observable shift. These measurements confirm electromagnetic coexistence of the mm-Wave readout link and the pixel sensor within the compact CEPC detector volume. Note that the RMS noise values quoted here are expressed in units of the threshold distribution's discriminator parameter; the absolute values reflect the TAICHU3 internal threshold DAC calibration.

V. MULTI-CHANNEL SYSTEM INTEGRATION AND TEST

A. System Architecture

To evaluate the scalability of the proposed approach to realistic detector readout scenarios, a multi-channel wireless transmission system was designed and fabricated. Fig. 9 presents the system block diagram. The system adopts a two-layer architecture (transmission and reception) without a relay stage, realizing to a direct inter-layer link.

The Transmission Layer consists of a Kintex-7 FPGA board providing data sourcing, a custom FMC adapter board for power distribution (12 V to 5 V DC-DC conversion), and six mm-Wave transmit modules mounted on flexible printed circuits. The Reception Layer mirrors this configuration with receive modules replacing the transmit modules and perform BER measurement.

Flexible printed circuit technology was employed for the mm-Wave module integration, with 0.3mm thickness, that is compliance in the curved detector electronics design. Each FPC strip has dimensions of 40 mm $\times$ 3 mm, carrying 5 V power and high-speed differential data signals. The six channels are arranged in a 2×3 planar array with a channel-to-channel pitch of 15 cm in the XY plane, and the transmission distance along the Z-axis ranges from 10 to 30 cm. All flexible PCBs are mounted on transparent acrylic sheets for support.

TABLE IV
MULTI-CHANNEL SYSTEM TRANSMISSION PERFORMANCE.

Per-Channel Rate	Active Channels	Aggregate Rate	BER
1.25 Gbps	6	7.5 Gbps	$<10^{-13}$
3.125 Gbps	6	18.75 Gbps	$<10^{-13}$
4 Gbps	4	16 Gbps	$<10^{-13}$
5 Gbps	2	10 Gbps	$<10^{-13}$

The adapter board use a standard 1.6 mm FR4 substrate with a four-layer stack-up, routes 12 V from the FMC HPC connector through a DC-DC converter to generate a regulated 5 V rail for the mm-Wave FPC.

B. Multi-Channel Transmission Performance

System-level BER testing was conducted at room temperature with transmission distances of 20 cm, evaluating both individual channel performance and parallel multi-channel operation. Table IV summarizes the results.

At per-channel data rates of 1.25 Gbps and 3.125 Gbps, all six channels achieved error-free transmission (BER $< 10^{-13}$) simultaneously, yielding an aggregated throughput of 7.5 Gbps and 18.75 Gbps, respectively. This single link rate exceeds the nominal ITK requirement of approximately 1.2 Gbps per stave, demonstrating that a single mm-Wave link can service multiple staves with bandwidth to spare, or alternatively that multi-channel aggregation can support higher-density readout configurations.

At 4 Gbps, the 4 channels with the shorter PCB trace lengths maintained error-free performance, while the remaining 2 channels—those with trace lengths exceeding 30 cm—exhibited eye closure due to frequency-dependent dielectric losses in the FPC substrate and could not establish reliable links. At 5 Gbps, only the channel with the shortest trace length (under 15 cm) achieved stable operation, while the remaining 4 channels failed to meet the BER criterion.

Fig. 10 presents eye diagram and IBERT results comparisons for three representative channels operating at 3.125

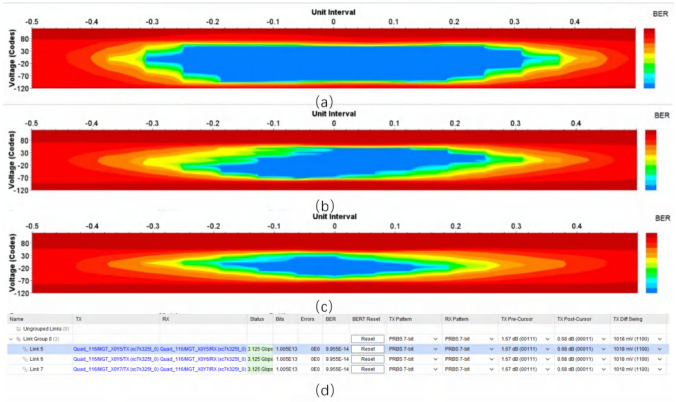

Fig. 10. Eye diagram comparison across three channels at 3.125 Gbps: (a) Channel 1 (short trace), (b) Channel 2 (medium trace), (c) Channel 3 (long trace). (d) All channels maintain BER $< 10^{-13}$.

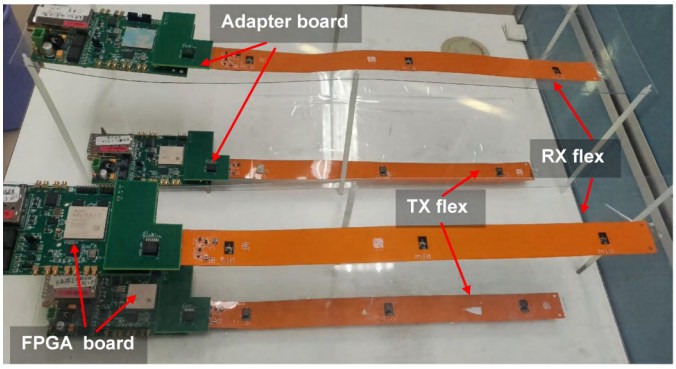

Fig. 11. Complete six-channel mm-Wave wireless transmission system. Transmission Layer (left) with six TX modules on FPC; Reception Layer (right) with six RX modules.

Gbps. Channel 1 (shortest trace, approximately 10 cm) exhibits a wide, clean eye opening with minimal jitter. Channel 2 (medium trace) shows a slightly reduced vertical opening but remains well within the receiver decision threshold. Channel 3 (longest trace, approximately 30 cm) displays noticeable amplitude reduction and increased edge jitter; however, with receiver equalization enabled, the BER remains below 10^{-13}.

C. Discussion

The multi-channel test results reveal a clear rate-versus-distance trade-off governed primarily by the PCB and FPC trace length on the digital side, rather than by the mm-Wave free-space link itself. At 3.125 Gbps and below, the system comfortably supports all six channels with BER performance meeting or exceeding typical high-energy physics data acquisition requirements (BER $< 10^{-13}$). The rate bottleneck at higher per-channel speeds can be addressed through several measures: (1) limiting the baseband trace length to under 15 cm; (2) introducing pre-emphasis at the transmitter and adaptive equalization at the receiver; and (3) adopting low-loss high-frequency substrate materials for the FPC in place of the standard polyimide.

The 18.75 Gbps aggregate throughput at 3.125 Gbps per channel confirms that the multi-channel architecture can deliver the necessary bandwidth for CEPC ITK readout with substantial headroom. The modular FPC-based design further enables flexible channel count scaling by simply replicating the mm-Wave transceiver modules and extending the FPC layout, without modifying the core FPGA or adapter board infrastructure.

VI. Conclusion

This paper has presented the development and experimental validation of a 60 GHz millimeter-wave wireless transmission system designed for the high-speed, low-material-budget readout of the CEPC Inner Tracker detector. The main achievements are as follows:

1) **Radiation tolerance verification:** The COTS ST60A2 60 GHz mm-Wave chip has been systematically tested under combined TID (X-ray, >5 Mrad) and NIEL (neutron, 1.2×10^{12} $n_{\text{eq}}/\text{cm}^2$) conditions. Stable communication performance was maintained throughout both irradiation campaigns, confirming the chip's suitability for the CEPC radiation environment and establishing a critical foundation for the engineering application of commercial mm-Wave technology in high-energy physics detectors.
2) **Enhanced transceiver module:** Link budget analysis identified the need for power amplification to bridge the 11–21 cm CEPC inter-layer spacing. The developed enhanced module, integrating ST60A2 with a PA and a PCB patch antenna in a 14 mm $\times$ 9 mm form factor, achieves a stable transmission distance of 45 cm at 5 Gbps with BER below 10^{-12}, representing an improvement over the unamplified case. The module exhibits no electromagnetic interference with the CEPC vertex detector prototype chip TAICHU3.
3) **Multi-channel integration:** A six-channel wireless transmission system was constructed using FPC technology, demonstrating an aggregated throughput of 18.75 Gbps (6×3.125 Gbps) over a 10–30 cm distance with BER below 10^{-13}.

The system satisfies all key requirements for CEPC ITK readout—high throughput, low material budget, radiation hardness, and modular scalability—and demonstrates the engineering viability of 60 GHz mm-Wave technology for next-generation particle physics experiments.

Future work will focus on: (1) optimizing the FPC layout and adopting low-loss substrate materials to extend the per-channel data rate to 5 Gbps and beyond; (2) investigating beamforming antenna arrays to improve link robustness against mechanical misalignment; and (3) conducting system-level integration tests with full-size ITK stave prototypes in a realistic detector environment.

Acknowledgments

This study was supported by the National Key Programme for S&T Research and Development (Grant No.: 2023YFA1606300). We also acknowledge the funding from the Innovation Fund of the Institute of High Energy Physics (Grant No.: E35456U2). We are grateful to the State Key

Laboratory of Particle Detection and Electronics for providing essential equipment support. We acknowledge the staff of the China Spallation Neutron Source (CSNS) for their support during the neutron irradiation campaign.

REFERENCES

[1] CEPC Study Group, "CEPC Technical Design Report – Reference Detector," IHEP-EP-2025-01, arXiv:2510.05260, 2025.

[2] H. K. Soltveit, R. Brenner, A. Schöning, and D. Wiedner, "Multi-gigabit wireless data transfer at 60 GHz," *J. Instrum.*, vol. 7, no. 12, p. C12019, 2012, doi: 10.1088/1748-0221/7/12/C12019.

[3] H. K. Soltveit, S. J. Dittmeier, A. Schöning, and D. Wiedner, "Towards multi-gigabit readout at 60 GHz for the ATLAS silicon microstrip detector," in *Proc. IEEE Nucl. Sci. Symp. Med. Imag. Conf. (NSS/MIC)*, Seoul, Korea, 2013, doi: 10.1109/NSSMIC.2013.6829448.

[4] S. Dittmeier, A. Schöning, H. K. Soltveit, and D. Wiedner, "Feasibility studies for a wireless 60 GHz tracking detector readout," *Nucl. Instrum. Methods Phys. Res. A*, vol. 817, pp. 164–174, 2016, doi: 10.1016/j.nima.2016.05.099.

[5] R. Brenner, "Status of development of technology for wireless data transfer in future tracking detectors," in *Proc. Topical Workshop on Electronics for Particle Physics (TWEPP-17)*, PoS(TWEPP-17), vol. 313, 2017.

[6] C. Dehos, E. Locci, R. Brenner, *et al.* (WADAPT Consortium), "Wireless allowing data and power transfer," in *Proc. TWEPP 2019*, PoS(TWEPP-2019)832, 2020. [Online]. Available: https://pos.sissa.it/390/832

[7] R. Brenner, C. Dehos, and E. Locci, "Multi gigabit wireless data transfer in detectors at future colliders," *Front. Phys.*, vol. 10, p. 872691, 2022, doi: 10.3389/fphy.2022.872691.

[8] J. Fu, *et al.*, "Mechanical design of an ultra-light vertex detector prototype for CEPC," *Radiat. Detect. Technol. Methods*, vol. 6, no. 2, pp. 159–169, 2022, doi: 10.1007/s41605-021-00310-4.

[9] S. K. Yong and C.-C. Chong, "An overview of multigigabit wireless through millimeter wave technology: potentials and technical challenges," *EURASIP J. Wireless Commun. Netw.*, vol. 2007, p. 78907, 2007, doi: 10.1155/2007/78907.

[10] STMicroelectronics, "ST60A2 — 60 GHz V-Band transceiver for short-range contactless connectivity," Data Brief, STMicroelectronics, 2023. [Online]. Available: https://www.st.com/en/wireless-connectivity/st60a2.html

[11] H. J. Liebe, "MPM — an atmospheric millimeter-wave propagation model," *Int. J. Infrared Millim. Waves*, vol. 10, no. 6, pp. 631–650, 1989, doi: 10.1007/BF01009565.

[12] W. Xu, H. Shi, H. Zhu, *et al.*, "Estimation of the radiation backgrounds in the CEPC vertex detector," *Radiat. Detect. Technol. Methods*, vol. 6, no. 2, pp. 170–178, 2022, doi: 10.1007/s41605-022-00320-w.

[13] Z. Yan *et al.*, "Readout electronics for the CEPC vertex detector prototype and beam telescope," *J. Instrum.*, vol. 18, no. 07, p. P07036, 2023, doi: 10.1088/1748-0221/18/07/P07036.